Available online at www.sciencedirect.com
SCIENCE DIRECT®

Journal of Solid State Chemistry 178 (2005) 3514–3521

JOURNAL OF SOLID STATE CHEMISTRY

www.elsevier.com/locate/jssc

New metal phosphonates containing coordination piperazine or pyridyl groups

Jun-Ling Song, Jiang-Gao Mao*

State Key Laboratory of Structural Chemistry, Fujian Institute of Research on the Structure of Matter, Chinese Academy of Sciences, Fuzhou 350002, P. R. China

Received 26 July 2005; received in revised form 2 September 2005; accepted 4 September 2005
Available online 7 October 2005

Abstract

Reactions of transition metal(II) salts with three aminophosphonic acids, 1-[$(H_2O_3PCH_2)_2NCH_2CH_2$–]-piperazine-4-$CH_2PO_3H_2$ (H_6L^1), 3-pyridyl-$CH_2N(CH_2PO_3H_2)_2$ (H_4L^2) and 4-pyridyl-$CH_2N(CH_2PO_3H_2)_2$ (H_4L^3) afforded three new metal phosphonates, namely, $Cu(H_4L^1)\cdot 2H_2O$ **(1)**, $Co(H_3L^2)_2\cdot H_2O$ **(2)** and $[Co(H_2L^3)(H_2O)]\cdot H_2O$ **(3)**. The structure of compound **1** features a 1D chain in which the CuN_2O_3 and CPO_3 polyhedra are interconnected by bridging phosphonate ligands to form 1D chains. Compound **2** has a layered structure. The cobalt(II) ions in the octahedral coordination geometries and $\{CPO_3\}$ tetrahedra are interconnected into an inorganic chain via –$N(CH_2PO_3H)_2$ moieties, and adjacent chains are further bridged by the coordination pyridyl groups of H_3L^2 into a 2D layer. The structure of compound **3** features a 2D double layered structure, in which the Co(II) ions are interconnected by bridging phosphonate groups into a 1D chain along *b*-axis. Neighboring chains are interconnected by coordination pyridyl groups into a double layer perpendicular to the *c*-axis.

Keywords: Hydrothermal syntheses; Crystal structures; Metal phosphonates; Inorganic–organic hybrids; Layered materials

1. Introduction

During the past two decades, considerable research efforts have been devoted to the synthesis of metal phosphonates with open-framework or microporous structures due to their interesting optical, ion-exchange, catalytic and sensing properties [1]. The strategy of attaching functional groups such as crown ether, amine, hydroxyl, and carboxylate groups to the phosphonic acid has proven to be effective for the isolation of a variety of metal phosphonates with open-framework and microporous structures [1–10]. Recently, a number of divalent metal compounds of substituted aminodiphosphonic acids, $RN(CH_2PO_3H_2)_2$ have been reported [2,11–13]. Results have shown that the organic substituent on the amine group plays a subtle role on the structures of metal phosphonates formed [11,12]. For example, $Cd(H_3L)_2$ ($H_4L = C_6H_5CH_2N(CH_2PO_3H_2)_2$) features double chains that are further interlinked by hydrogen bonds. With one more CH_2– group between the phenyl and the amine group, $Cd(H_3L')_2$ ($H_4L' = C_6H_5CH_2CH_2N(CH_2PO_3H_2)_2$) has a layered structure [11a]. However, metal complexes of $RN(CH_2PO_3H_2)_2$ ligands bearing additional coordination pyridyl or piperazine groups are rather rare [14,15]. The additional piperazine or pyridyl group on the ligands may serve as pH mediator as well as coordination atoms for the metal ions. Moreover, isomerization of such ligands may result in metal phosphonates with different structure types. To further our knowledge on these compounds, we have synthesized three phosphonate ligands with piperazine or pyridyl groups (see Scheme 1). Hydrothermal reactions of the above ligands with metal salts afforded three new metal(II) phosphonates, namely $Cu(H_4L^1)\cdot 2H_2O$ **(1)**, $Co(H_3L^2)_2\cdot H_2O$ **(2)** and $[Co(H_2L^3)(H_2O)]\cdot H_2O$ **(3)**, in which the piperazine or pyridyl group is involved in metal coordination. Herein we report their syntheses and crystal structures.

---

*Corresponding author. Fax: +86 591 3714946.
E-mail address: mjg@ms.fjirsm.ac.cn (J.-G. Mao).

0022-4596/$ - see front matter © 2005 Elsevier Inc. All rights reserved.
doi:10.1016/j.jssc.2005.09.001

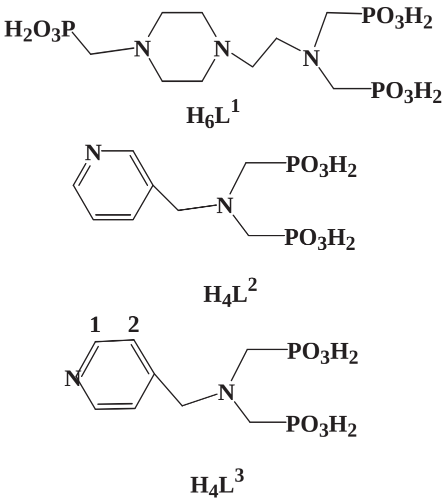

Scheme 1. Structure of H_6L^1, H_4L^2 and H_4L^3.

2. Experimental section

2.1. Materials and methods

All chemicals were obtained from commercial sources and used without further purification. Elemental analyses were performed on a Vario EL III elemental analyzer. Thermogravimetric analyses were carried out on a NETZSCH STA 449C unit at a heating rate of 15 °C/min under an oxygen atmosphere. IR spectra were recorded on a Magna 750 FT-IR spectrometer as KBr pellets in the 4000–400 cm^{-1}. ^{1}H and ^{31}P NMR spectra were recorded on a Varian Unity 500 NMR in D_2O solvent. H_3PO_4 (85%) was used as ^{31}P standard reference.

2.2. Synthesis of H_6L^1, H_4L^2 and H_4L^3

H_6L^1 and H_4L^2 were prepared by a Mannich-type reaction according to procedures previously described [15]. H_4L^3, which is an isomer of H_4L^2, was prepared in a yield of 34.6% by a Mannich-type reaction of 4-(aminomethyl) pyridine (100 mmol, 12.6 ml), 16 ml of hydrochloric acid, 20 ml of deionized water, phosphorous acid (400 mmol, 32.8 g) and paraformaldehyde (300 mmol, 9 g) according to the procedures used for the synthesis of H_4L^2 [16]. ^{31}P NMR spectroscopy shows a single peak at $\delta = 10.71$ ppm. ^{1}H NMR: 3.50 ppm (N–CH_2–PO_3, d, 4H, $J_{H,P} = 12.5$ Hz), 4.90 ppm (pyridine–CH_2–N, s, 2 H), 8.31 ppm [C(2)H, 1H, s], 8.92 ppm [C(1)H, d, $J_{H,H} = 8.5$ Hz] (see Scheme 1 for the labeling of the carbon atoms). $C_8H_{14}N_2O_6P_2$: calcd. C 32.45, H 4.76, N 9.46; found C 32.53, H 4.98, N 9.23. IR (KBr, cm^{-1}): 3392m, 3342m, 3016m, 3016m, 1662w, 1629w, 1521w, 1458m, 1433m, 1383w, 1271m, 1174s, 1119vs, 1057m, 1024m, 992m, 952m, 936w, 776w, 556m, 464w.

2.3. Synthesis of Cu (H_4L^1) · $2H_2O$ (**1**)

A mixture of $Cu(NO_3)_2 \cdot 3H_2O$ (0.26 g, 1.0 mmol) and H_6L^1 (0.20 g, 0.5 mmol) in 10 ml of distilled water was strongly stirred and the pH value of the resultant solution was adjusted to approximately 4 by slow addition of $(C_4H_9)_4NOH$. The resultant blue solution was filtered off and ethanol was allowed to diffuse into slowly at room temperature. After several weeks, blue brick crystals of compound **1** were collected in 46% yield (based on copper). The final pH value of the solution is 4.5. Elemental analysis for **1**: Calc. for $C_9H_{26}CuN_3O_{11}P_3$: C 21.25, H 5.15, N 8.26%. Found: C 20.90, H 5.43, N 8.32%. IR (KBr, cm^{-1}): 3350m, 3003w, 2738m, 2347w, 1651w, 1468w, 1157vs, 1133m, 1050s, 1025s, 965m, 919m, 769w, 567m, 537w, 432w.

2.4. Synthesis of Co (H_3L^2)$_2$ · H_2O (**2**)

A mixture of $CoCl_2 \cdot 6H_2O$ (0.24 g, 1.0 mmol) and H_4L^2 (0.15 g, 0.5 mmol) in 10 ml of distilled water was sealed into a bomb equipped with a Teflon liner (25 ml), and then heated at 130 °C for 5 days. Pink crystals of **2** were collected in 50% yield (based on cobalt). The initial and final pH values of the solution are 3.0 and 3.5, respectively. Elemental analysis for **2**: Calc. for $C_{16}H_{30}CoN_4O_{14}P_4$: C 28.04, H 4.41, N 8.18%. Found: C 27.96, H 4.53, N 8.24%. IR (KBr, cm^{-1}): 3416s, 2953m, 2334m, 1622m, 1606m, 1486w, 1427m, 1271m, 1197s, 1077vs, 1034s, 991w, 940m, 914s, 786w, 704m, 583m, 540w, 477w, 442m.

2.5. Synthesis of Co (H_2L^3)(H_2O) · H_2O (**3**)

A mixture of $Co(CH_3COO)_2 \cdot H_2O$ (0.22 g, 1.0 mmol) and H_4L^3 (0.15 g, 0.5 mmol) in 10 ml of distilled water was sealed into a bomb equipped with a Teflon liner (25 ml), and then heated at 180 °C for 4 days. The pH value of the resultant solution was adjusted to approximately 3.0 by slow addition of 1 M NaOH solution. Pink crystals of **3** were collected in about 6% yield (based on cobalt). The final pH value is about 4.0. Elemental analysis for **3**: Calc. for $C_8H_{16}CoN_2O_8P_2$: C 24.69, H 4.14, N 7.20%. Found: C 23.54, H 4.56, N 6.92%. IR (KBr, cm^{-1}): 3367m, 3256m, 2893w, 2342w, 1619m, 1434w, 1401w, 1272w, 1198m, 1140vs, 1108s, 1077vs, 1057s, 1023w, 952w, 940w, 922w, 899w, 795w, 734m, 636m, 582m, 470m.

2.6. Crystallography

Single crystals of **1, 2** and **3** were mounted on a Siemens Smart CCD (for **2**) or Rigaku Mercury CCD (for **1** and **3**) diffractometer equipped with a graphite-monochromated MoKα radiation ($\lambda = 0.71073$ Å). Intensity data were collected by the narrow frame method at 293 K. The data sets were corrected for Lorentz and polarization as well as for absorption by ψ scan technique for compound **2** or Multi-Scan method for compounds **1** and **3** [17a]. All three structures were solved by direct methods and refined by full-matrix least-squares fitting on F^2 by SHELX-97 [17b]. All non-hydrogen atoms were refined with anisotropic thermal parameters. O(2 w) and O(3 w) of compound **3** with larger thermal parameters were refined with 50% occupancy. All hydrogen atoms attached to the carbon atoms were located at geometrically calculated positions, so are those for the protonated phosphonate groups and amine groups. The hydrogen atoms of the water molecule in compound **2** were located from difference Fourier maps, and those of water molecules in compounds **1** and **3** were not included in the refinements. Crystallographic data and structural refinements are summarized in Table 1. Important bond distances and angles are listed in Tables 2, respectively, for compounds **1**, **2** and **3**.

CCDC-265380, 265381 and 265382 contain the supplementary crystallographic data for this paper. These data can be obtained free of charge at www.ccdc.cam.ac.uk/conts/retrieving.html [or from the Cambridge Crystallographic Data Centre, 12, Union Road, Cambridge CB2 1EZ, UK; Fax: (internat.) +44 1223/336 033; *E-mail address*: deposit@ccdc.cam.ac.uk.

3. Results and discussion

Compound **1** features a 1D chain structure. There are one unique Cu(II) ion, one H_4L^1 ligand and two lattice water molecules in the asymmetric unit, as shown in Fig. 1. Cu(1) atom is in a distorted square pyramidal coordination environment. Four coordination sites are provided by a tetradentate chelating H_4L^1 ligand (O(12), O(22), N(1), N(2)) and the fifth one (O(31a)) (symmetry code: $-\frac{1}{2}+x, y, \frac{1}{2}-z$) comes from a phosphonate group of another H_4L^1 ligand. O(12), O(22), O(31a) and N(1) atoms form a square plane with a mean deviation of 0.167 Å, whereas N(2) occupies the apical position. The Cu–O (1.937(3)–1.968(3) Å) and Cu–N (2.088(3)–2.318(3) Å) distances are comparable to those reported for other copper(II) aminophosphonates [2a,4d,18]. Each H_4L^1 ligand is penta-dentate (Scheme 2a), it chelates with a copper(II) ion in a tetradentate fashion (2N and 2O) and bridges to another copper(II) ion (Fig. 1). All three phosphonate groups of the phosphonate ligand are unidentate and singly protonated (O(11), O(20) and O(32)). N(2) atom of the piperazine ring is unidentate whereas N(3) is singly protonated and remains non-coordinated.

The CuN_2O_3 and CPO_3 polyhedra are interconnected by bridging phosphonate ligands into a 1D zigzag chain (Fig. 2). These 1D chains are further interlinked via hydrogen bonds among non-coordination phosphonate oxygen atoms and amine group as well as lattice water molecules into a 3D network (Fig. 3).

Compound **2** with a M/L ratio of 1:2 features a layer structure. There is one unique Co(II) ion in the asymmetric unit (Fig. 4). Co(1) located at a center of symmetry is octahedrally coordinated by four phosphonate oxygens from four H_3L^2 ligands and two pyridyl nitrogen atoms from two additional H_3L^2 ligands. The Co–O bond lengths range from 2.065(2)–2.193(2) Å and the Co–N bond lengths are 2.144(2) Å. These bond distances are comparable to those in other Co(II) aminophosphonates [12a,19]. The H_3L^2 ligand is tridentate, bridging to three cobalt atoms by using two phosphonate oxygens from two

Table 1
Crystal data and structure refinements for compounds **1**, **2** and **3**

Compound	**1**	**2**	**3**
Formula	$C_9H_{26}CuN_3O_{11}P_3$	$C_{16}H_{30}CoN_4O_{14}P_4$	$C_8H_{16}CoN_2O_8P_2$
fw	508.78	685.25	389.10
Space group	*Pbca*	$P\bar{1}$	*C2/c*
a (Å)	12.039	8.8156(18)	15.9621(16)
b (Å)	14.213	8.9345(18)	9.681
c (Å)	21.6320(13)	9.2350(18)	19.228(2)
α (deg.)	90.00	81.75(3)	90.00
β (deg.)	90.00	73.67(3)	101.783(5)
γ (deg.)	90.00	67.65(3)	90.00
V (Å^3)	3701.5(2)	645.0(2)	2908.8(5)
Z	8	1	8
D_{calcd} (g cm^{-3})	1.826	1.764	1.777
μ (mm^{-1})	1.501	0.990	1.439
Total reflections	21427	5027	8642
Independent reflections	3267 ($R_{int} = 0.0452$)	2734 ($R_{int} = 0.0318$)	2556 ($R_{int} = 0.0205$)
Parameters refined	244	186	194
GOF on F^2	1.234	1.057	1.059
R_1, wR_2 ($I > 2(I)$)[a]	0.0533/0.1083	0.0415/0.0869	0.0388/0.1112
R_1, wR_2 (all data)	0.0581/0.1105	0.0546/ 0.0911	0.0411/0.1132

[a] $R_1 = \sum ||Fo| - |Fc|| / \sum |Fo|$, w$R_2 = \{\sum w[(Fo)^2 - (Fc)^2]^2 / \sum w[(Fo)^2]^2\}^{1/2}$.

Table 2
Selected bond lengths (Å) and angles (°) for compounds **1**, **2** and **3**

Compound **1**			
Cu(1)–O(12)	1.937(3)	Cu(1)–O(22)	1.968(3)
Cu(1)–O(31)#1	1.945(3)	Cu(1)–N(1)	2.088(3)
Cu(1)–N(2)	2.318(3)	P(1)–O(10)	1.480(4)
P(1)–O(11)	1.568(4)	P(1)–O(12)	1.501(3)
P(2)–O(20)	1.547(3)	P(2)–O(21)	1.494(3)
P(2)–O(22)	1.528(3)	P(3)–O(30)	1.491(3)
P(3)–O(31)	1.501(3)	P(3)–O(32)	1.552(3)
Hydrogen bonds			
O(1 w)…O(32)	2.512(5)	O(2 w)…O(10)#2	2.715(5)
O(1 w)…O(2 w)	2.694(6)	O(2 w)…O(10)#3	2.760(7)
N(3)…O(22)#4	2.771(4)		
Compound **2**			
Co(1)–O(12)#1	2.065(2)	Co(1)–O(12)#2	2.065(2)
Co(1)–N(1)	2.144(2)	Co(1)–N(1)#3	2.144(2)
Co(1)–O(22)#4	2.193(2)	Co(1)–O(22)#5	2.193(2)
P(1)–O(11)	1.499(2)	P(1)–O(12)	1.507(2)
P(1)–O(13)	1.578(2)	P(2)–O(21)	1.492(2)
P(2)–O(22)	1.515(2)	P(2)–O(23)	1.574(2)
Hydrogen bonds			
O(1w)…O(11)	2.759(3)	O(1w) …O(23)#6	2.612(3)
N(2)…O(21)#1	2.658(3)	N(2)–H(2b) …O(21)#1	151.1
Compound **3**			
Co(1)–O(13)	2.074(2)	Co(1)–N(1)#2	2.125(3)
Co(1)–O(22)	2.055(2)	Co(1)–O(1W)	2.171(3)
Co(1)–O(23)#1	2.108(2)	Co(1)–N(2)	2.253(3)
P(1)–O(11)	1.511(3)	P(2)–O(21)	1.584(2)
P(1)–O(12)	1.558(2)	P(2)–O(22)	1.511(2)
P(1)–O(13)	1.516(3)	P(2)–O(23)	1.496(2)
Hydrogen bonds			
O(1W)…O(3W)	2.650(9)	O(2W)…O(3W)	2.86(3)
O(12)…O(11)#3	2.568(3)	O(21)…O(11)#4	2.662(3)
O(12)–H(2b)…O(11)#3	167.4	O(21)–H(4b)…O(11)#4	178.6

Symmetry transformations used to generate equivalent atoms:
For **1**: #1 $x-\frac{1}{2}, y, -z+\frac{1}{2}$; #2 $x, -y+\frac{3}{2}, z-\frac{1}{2}$; #3 $-x+1, y+\frac{1}{2}, -z+\frac{1}{2}$; #4 $x+\frac{1}{2}, y, -z+\frac{1}{2}$.
For **2**: #1 $-x$, $-y+1$, $-z$; #2 $x+1$, y, z; #3 $-x+1, -y+1$, $-z$; #4 $x+1$, $y-1$, z; #5 $-x$, $-y+2$, $-z$; #6 $-x$, $1-y$, $-1-z$.
For **3**: #1 $-x+\frac{3}{2}, y+\frac{1}{2}, -z+\frac{3}{2}$; #2 $x+\frac{1}{2}, y+\frac{1}{2}, z$; #3 $-x, 2-y, 1-z$; #4 $-x+\frac{1}{2}, y-\frac{1}{2}, -z+\frac{3}{2}$.

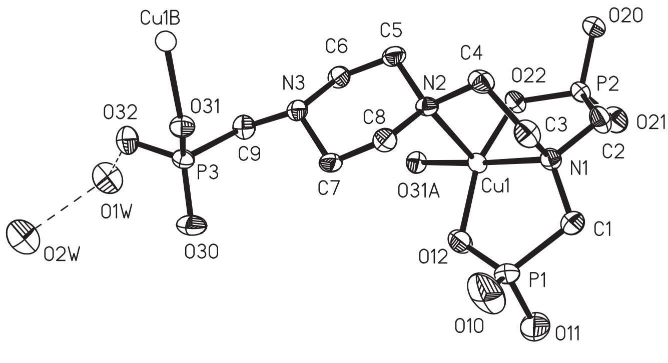

Fig. 1. ORTEP representation of the selected unit of compound **1**. The thermal ellipsoids are drawn at 50% probability. Hydrogen bonds are drawn as dashed lines. Symmetry codes for generated atoms: (a) $-\frac{1}{2}+x, y, \frac{1}{2}-z$; (b) $\frac{1}{2}+x, y, \frac{1}{2}-z$;

phosphonate groups and the pyridyl nitrogen atom (Scheme 2b). The amino group (N(2)) and the two phosphonate groups are singly protonated (O(13) and O(23)) based on charge balance and P–O distances (Table 2).

The CoN_2O_4 octahedra are interconnected by bridging phosphonate ligands into a (001) layer (Fig. 5). Such connectivity leads to 18 member rings composed of Co–(N–C–C–C–N–C–P–O)$_2$–Co and 16 member rings containing Co–(O–P–C–N–C–P–O)$_2$–Co. Such 2D layer can also be viewed as 1D chains formed by Co(II) ions and –N(CH_2PO_3H)$_2$ moieties are further cross-linked by Py–CH_2– groups. Within the 2D layer, the protonated amine group (N(2)) is hydrogen bonded with the non-coordination phosphonate oxygen (O(21)) from another ligand. The hydrogen bond N(2)–H(2B)…O(21) has a D…A distance of 2.658(3) Å and D–H…A angle of 151.1°. These layers are further interlinked via hydrogen bonds among non-coordinated phosphonate oxygen atoms and lattice water molecules into a 3D network (Table 2, Fig. 6).

Though H_4L^2 and H_4L^3 are isomers and differs only from the position of the pyridyl group, the structures of their Co(II) compounds are quite different. Compound **3** with a M/L ratio of 1:1 features a two-dimensional double layer. As shown in Fig. 7, Co(1) is octahedrally coordinated by a H_2L^3 ligand in a tridentate chelating fashion (O(13), N(2), O(22)), a phosphonate oxygen and a pyridyl nitrogen atoms from two other H_2L^3 ligands as well as an aqua ligand. The Co–O bond lengths fall in the range 2.055(2)–2.171(3) Å and the Co–N bond lengths fall in the range 2.125(3)–2.253(3) Å, these bond distances are comparable to those of compound **2**. Unlike the tridentate bridging H_3L^2 ligand in compound **2**, the H_2L^3 ligand in compound **3** acts as a pentadentate chelating and bridging ligand. It chelates with a Co (II) in a tridentate fashion (2O and 1N) and also bridges with two other Co (II) ions by using a phosphonate oxygen and the pyridyl group (Scheme 2c). $P(2)O_3$ group is bidentate bridging whereas $P(1)O_3$ is unidentate. Both phosphonate groups are singly protonated (O(12) and O(21)) based on P–O distances (Table 2).

The interconnection of Co(II) ions in compound **3** by bridging $P(2)O_3$ groups resulted in a 1D chain along *b*-axis. Neighboring such chains are further cross-linked by the organic groups of H_2L^3 anions into a 2D double layer parallel to the *ab* plane, the unidentate $P(1)O_3$ groups act as pendent groups (Fig. 8). Within the double layer, hydrogen bonds are formed between non-coordination phosphonate oxygen atoms. The D…A contact and D–H…A angle for hydrogen bond O(21)–H(4b)…O(21) (symmetry code: $\frac{1}{2}-x, y-\frac{1}{2}, \frac{3}{2}-z$) are 2.662(3) Å and 178.6°, respectively. These double layers are further interconnected into a 3D network via interlayer hydrogen bonds among non-coordination phosphonate oxygen atoms, aqua ligand and lattice waters (Fig. 9, Table 2). It is worthy to mention that the hydrogen bond formed between non-coordination

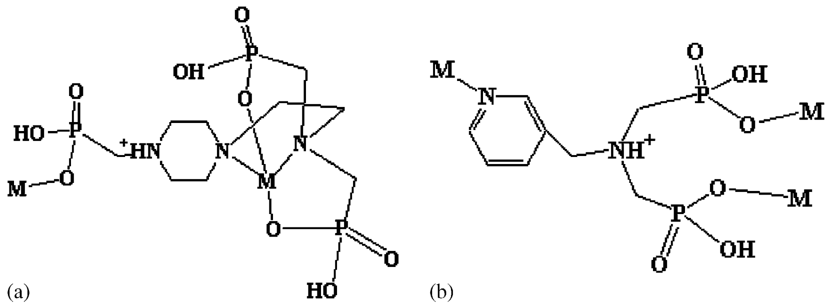

Scheme 2. Coordination modes of phosphonate ligands in compounds **1** (a), **2** (b), and **3** (c).

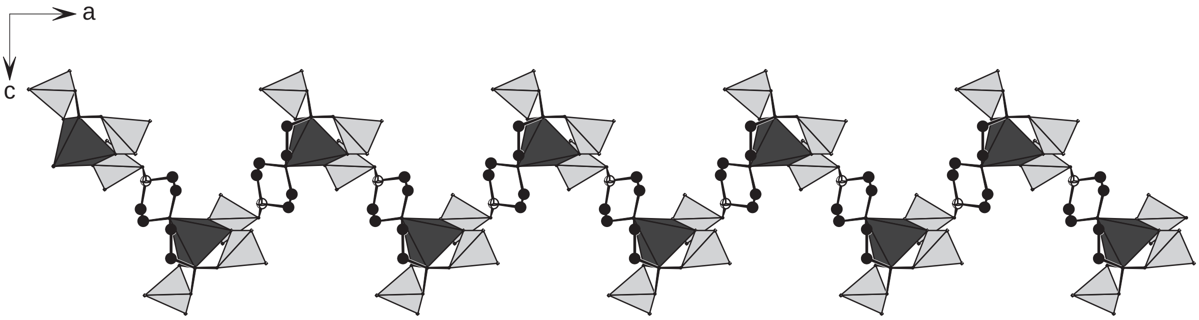

Fig. 2. A 1D zigzag chain structure along *a*-axis in compound **1**. The CuN_2O_3 and $C–PO_3$ polyhedra are shaded in dark and light gray, respectively. C and N atoms are drawn as black and octanded circles, respectively.

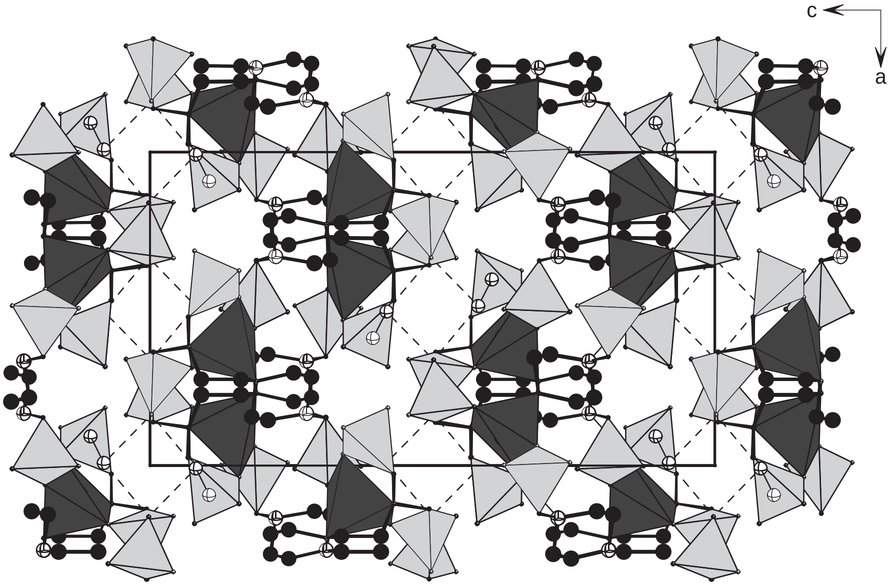

Fig. 3. View of structure of compound **1** along *b*-axis. The CuN_2O_3 and $C–PO_3$ polyhedra are shaded in dark and light gray, respectively. C, O and N atoms are drawn as black, crossed and octanded circles, respectively. Hydrogen bonds are represented by dashed lines.

phosphonate oxygen atoms (O(12)–H(2b)…O(11), symmetry code: $-x$, $2-y$, $1-z$) is very strong with D…A distance of 2.568(3) Å and D–H…A angle of 178.6° (Table 2).

The TGA diagram of **1** reveals three main steps of weight losses. The first step corresponds to the loss of two lattice water molecules. The weight loss begins at 86 °C and is completed at 201 °C. The observed weight loss of 7.1% is

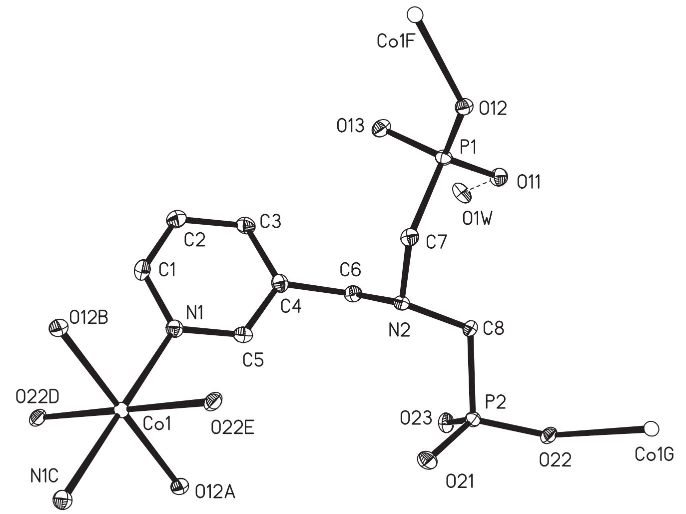

Fig. 4. ORTEP representation of the asymmetric unit of compound **2**. Symmetry codes for generated atoms: (a) $-x, -y, -z$; (b) $x+1, y, z$; (c) $-x+1, -y, -z$; (d) $-x, -y+1, -z$; (e) $x+1, y-1, z$; (f) $x-1, y, z$; (g)$x-1, y+1, z$.

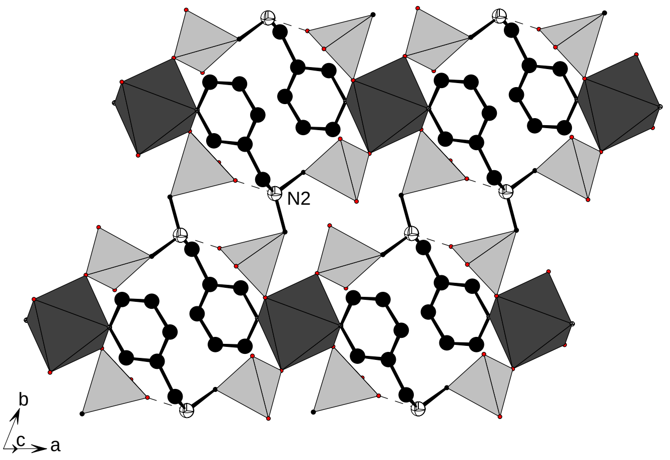

Fig. 5. A (001) 2D metal phosphonate layer in **2**. The CoN_2O_4 octahedra and C–PO_3 tetrahedra are shaded in dark and light gray, respectively. C and N atoms are drawn as black and octanded circles, respectively. Hydrogen bonds are represented by dashed lines.

very close to the calculated value (7.8%). The second weight loss occurs in the range of 223–631 °C, which can be attributed to the combustion of organic groups. The third step corresponds to further decomposition of the phosphonate ligands. The total weight loss at 1000 °C is 64.5% and the residual was not identified due to its corrosion with the container (Al_2O_3 crucible). The TGA diagram of **2** also indicates three main steps of weight losses. The first step from 67 °C to 173 °C corresponds to the release of lattice water molecule. The observed weight loss of 2.1% is slightly less than the calculated value (2.6%). The second weight change occurs the temperature range of 238–672 °C, which corresponds to the loss of water molecules formed by the condensation of hydrogen phosphonate groups and partial combustion of organic groups. The third step overlapping with the second one corresponds to the further decomposition of organic groups. The total weight loss at

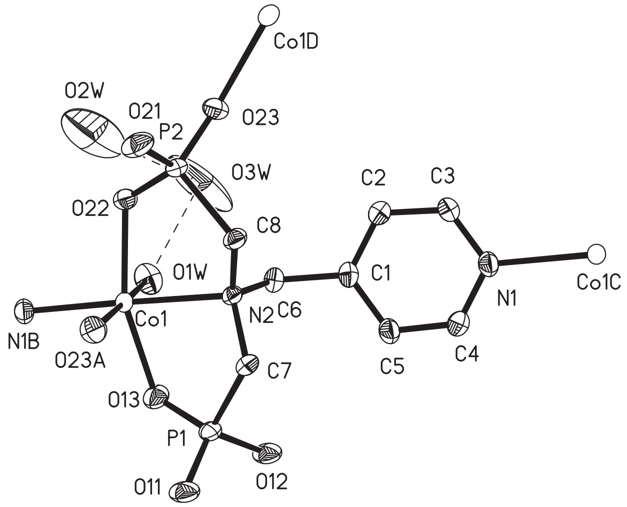

Fig. 7. ORTEP representation of the asymmetric unit of compound **3**. Symmetry codes for the generated atoms: (a) $\frac{3}{2}-x, -\frac{1}{2}+y, \frac{3}{2}-z$; (b) $-\frac{1}{2}+x, -\frac{1}{2}+y, z$; (c) $\frac{1}{2}+x, \frac{1}{2}+y, z$; (d) $\frac{3}{2}-x, \frac{1}{2}+y, \frac{3}{2}-z$.

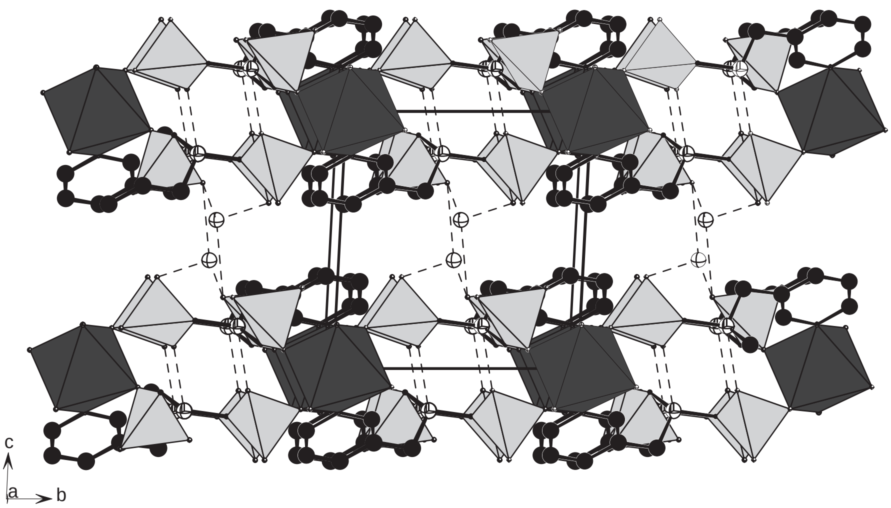

Fig. 6. View of the structure of **2** down the *a*-axis. The CoN_2O_4 octahedra and C–PO_3 tetrahedra are shaded in dark and light gray, respectively. C, O and N atoms are drawn as black, crossed and octanded circles, respectively. Hydrogen bonds are represented by dashed lines.

1000 °C is 56.8% and the residual was also not identified due to its corrosion with the container (Al_2O_3 crucible). TGA study for compound **3** was not performed due to insufficient sample available.

4. Conclusion

In summary, three new metal(II) phosphonates containing coordination piperazine or pyridyl group have been reported. The piperazine group in compound **1** involves in both metal coordination and hydrogen bonding. The pyridyl groups in compounds **2** and **3** are coordinated with the metal centers. Compound **1** is 1D whereas compounds **2** and **3** are layered. The different layered structures of compounds **2** and **3** are probably mainly due to the different coordination modes of the two isomeric phosphonate ligands adopted and the different pH values of reaction media. The higher pH value for the preparation of **3** allows the amine group of the phosphonate ligand to be deprotonated, therefore the amine group and phosphonate groups can chelate with a cobalt(II) ion. The different charges on the two different phosphonate ligands also leads to different M/L ratios for compounds **2** and **3**. Future research efforts will be devoted to the more systematic studies of metal aminophosphonates containing other N-donor groups.

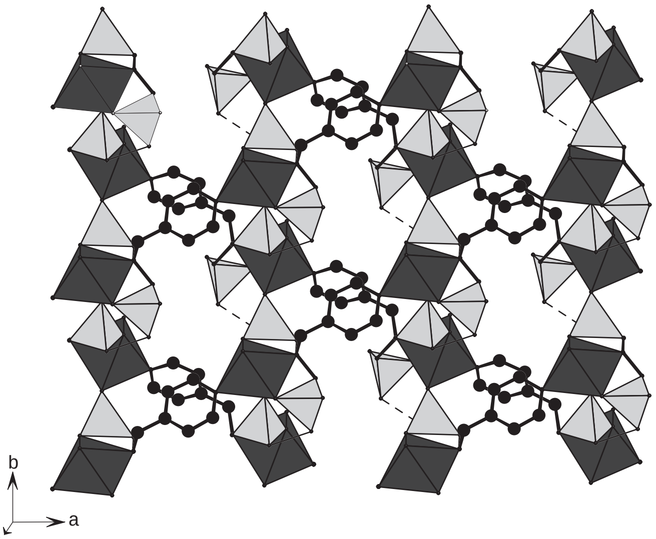

Fig. 8. A 2D double metal phosphonate layer in compound **3**. CoN_2O_4 octahedra and C-PO_3 tetrahedra are shaded in dark and light gray, respectively. C atoms are represented by black circles. Hydrogen bonds are drawn as dotted lines.

Acknowledgments

This work was supported by the National Natural Science Foundation of China (20371047) and NSF of Fujian Province (E0420003).

Appendix A. Supplementary materials

Supplementary data associated with this article can be found in the online version at doi:10.1016/j.jssc.2005.09.001.

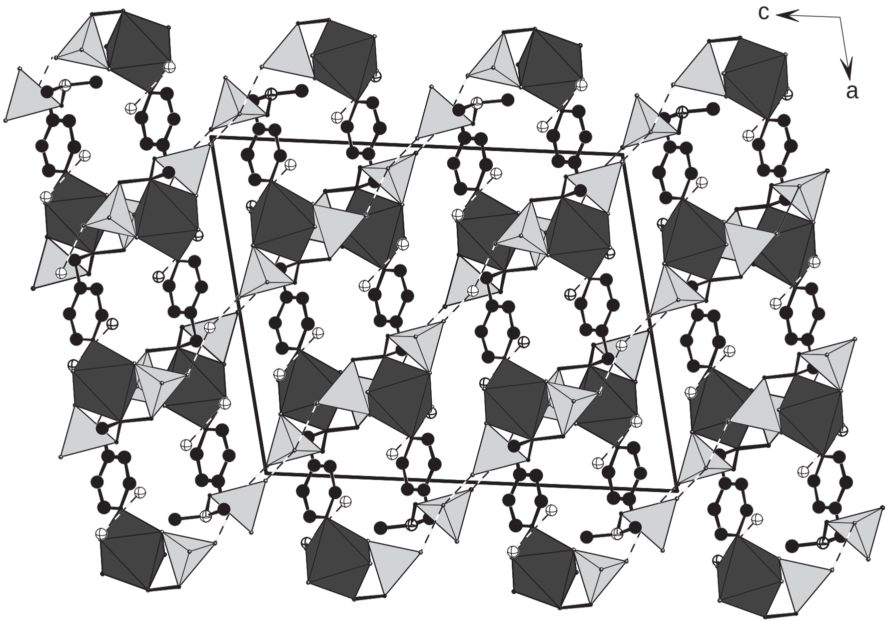

Fig. 9. View of the crystal structure of **3** down the *b*-axis. CoN_2O_4 octahedra and C–PO_3 tetrahedra are shaded in dark and light gray, respectively. C, O and N atoms are drawn as black, crossed and octanded circles, respectively. Hydrogen bonds are represented by dashed lines.

References

[1] (a) A. Clearfield, Metal phosphonate chemistry, in: K.D. Karlin (Ed.), Progress Inorganic Chemistry, Vol. 47, Wiley, New York, 1998, pp. 371–510 (and references therein);
 (b) A.K. Cheetham, G. Férey, T. Loiseau, Angew. Chem. Int. Ed. 38 (1999) 3268;
 (c) J. Zhu, X. Bu, P. Feng, G.D. Stucky, J. Am. Chem. Soc. 122 (2000) 11563;
 (d) A. Clearfield, Cur. Opin. Solid State. Mater. 6 (2002) 495 (and references therein).

[2] (a) J.-G. Mao, Z.K. Wang, A. Clearfield, Inorg. Chem. 41 (2002) 3713;
 (b) J.-G. Mao, Z.K. Wang, A. Clearfield, Inorg. Chem. 41 (2002) 2334;
 (c) J.-G. Mao, Z.K. Wang, A. Clearfield, Inorg. Chem. 41 (2002) 6106;
 (d) J.-G. Mao, Z.K. Wang, A. Clearfield, J. Chem. Soc., Dalton Trans. (2002) 4457.

[3] (a) B. Zhang, A. Clearfield, J. Am. Chem. Soc. 119 (1997) 2751;
 (b) A. Clearfield, C.V.K. Sharma, B. Zhang, Chem. Mater. 13 (2001) 3099;
 (c) C. Sassoye, K. Norton, S.C. Sevov, Inorg. Chem. 42 (2003) 1652;
 (d) N. Stock, T. Bein, Angew. Chem. Int. Ed. 43 (2004) 749.

[4] (a) Y.-D. Chang, J. Salta, J. Zubieta, Angew. Chem. Int. Ed. 33 (1994) 325;
 (b) E.I. Tolis, M. Helliwell, S. Langley, J. Raftery, R.E.P. Winpenny, Angew. Chem., Int. Ed. 42 (2003) 3804;
 (c) S.O.H. Gutschke, D.J. Price, A.K. Powell, P.T. Wood, Angew. Chem., Int. Ed. 40 (2001) 1920;
 (d) D.-Y. Kong, Y. Li, J.H. Ross, A. Clearfield, Chem. Commun. (2003) 1720;
 (e) V. Chandrasekhar, S. Kingsley, B. Rhatigan, M.K. Lam, A.L. Rheingold, Inorg. Chem. 41 (2002) 1030.

[5] (a) O.R. Evans, H.L. Ngo, W.B. Lin, J. Am. Chem. Soc. 123 (2001) 10395;
 (b) C. Serre, N. Stock, T. Bein, G. Férey, Inorg. Chem. 43 (2004) 3159.

[6] (a) N. Stock, S.A. Frey, G.D. Stucky, A.K. Cheetham, J. Chem. Soc. Dalton Trans. (2000) 4292;
 (b) N. Stock, T. Bein, J. Solid State Chem. 167 (2002) 330;
 (c) N. Stock, M. Rauscher, T. Bein, J. Solid State Chem. 177 (2004) 642.

[7] M.A. Petruska, B.C. Watson, M.W. Meisel, D.R. Talham, Chem. Mater. 14 (2002) 2011.

[8] (a) E.K. Brechin, R.A. Coxall, A. Parkin, S. Parsons, P.A. Tasker, R.E.P. Winpenny, Angew. Chem. Int. Ed. 40 (2001) 2700;
 (b) H.-H. Song, P. Yin, L.-M. Zheng, J.D. Korp, A.J. Jacobson, S. Gao, X.-Q. Xin, J. Chem. Soc., Dalton Trans. (2002) 2752.

[9] A. Cabeza, X. Ouyang, C.V.K. Sharma, M.A.G. Aranda, S. Bruque, A. Clearfield, Inorg. Chem 41 (2002) 2325.

[10] D.M. Poojary, B. Zhang, A. Clearfield, J. Am. Chem. Soc. 119 (1997) 12250.

[11] (a) Z.-M. Sun, B.-P. Yang, Y.-Q. Sun, J.-G. Mao, A. Clearfield, J. Solid State Chem. 176 (2003) 62;
 (b) Z.-M. Sun, J.-G. Mao, Y.-Q. Sun, H.-Y. Zeng, A. Clearfield, New J. Chem. 27 (2003) 1326;
 (c) Z.-M. Sun, J.-G. Mao, B.-P. Yang, S.-M. Ying, Solid State Sci 6 (2004) 295;
 (d) Z.-M. Sun, J.-G. Mao, Z.-C. Dong, Polyhedron 24 (2005) 571.

[12] (a) S.-M. Ying, J.-G. Mao, J. Mol. Struct. 748 (2005) 63;
 (b) S.-M. Ying, J.-G. Mao, Eur. J. Inorg. Chem. (2004) 1270;
 (c) S.-M. Ying, J.-G. Mao, B.-P. Yang, Z.-M. Sun, Inorg. Chem. Commun. 6 (2003) 1319.

[13] (a) B.I. Makaranets, T.N. Polynova, N.D. Mitrofanova, M.A. Porai-Koshits, J. Struct. Chem. 32 (1991) 94;
 (b) A. Turner, P.A. Jaffres, E.J. MacLean, D. Villemin, V. McKee, G.B. Hix, Dalton Trans. (2003) 1314;
 (c) N. Stock, Solid State Sci. 4 (2002) 1089;
 (d) U. Costantino, M. Nocchetti, R. Vivani, J. Am. Chem. Soc. 124 (2002) 8428.

[14] (a) P. Ayyappan, O.R. Evans, B.M. Foxman, K.A. Wheeler, T.H. Warren, W.B. Lin, Inorg. Chem. 40 (2001) 5954;
 (b) P. Ayyappan, O.R. Evans, Y. Cui, K.A. Wheeler, W.B. Lin, Inorg. Chem. 41 (2002) 4978.

[15] (a) J.L. Song, J.-G. Mao, Y.Q. Sun, A. Clearfield, Eur. J. Inorg. Chem. (2003) 4218;
 (b) S.W.A. Bligh, N. Choi, S. Failla, P. Finocchiaro, A. Iyasov, M. Libertini, C.M. McGrath, M. MaPartlin, T.M. Woodroffe, J. Chem. Soc., Dalton Trans. (1994) 3333.

[16] K. Moedritzer, R.R. Irani, J. Org. Chem. 31 (1966) 1603.

[17] (a) CrystalClear version 1.3.5. Rigaku Corp., Woodlands, TX, 1999;
 (b) G.M. Sheldrick, SHELXTL, Crystallographic Software Package, version 5.1, Bruker-AXS, Madison, WI, 1998.

[18] (a) K.P. Guerra, R. Delgado, L.M.P. Lima, M.G.B. Drew, V. Felix, Dalton Trans. (2004) 1812;
 (b) F. Cecconi, C.A. Ghilardi, P.A.L. Luis, S.M. Midollini, A. Orlandini, D. Dakternieks, A. Duthie, S. Dominguez, E. Berti, A. Vacca, J. Chem. Soc., Dalton Trans. (2001) 211;
 (c) J. Kotek, P. Lubai, P. Hermann, I. Cisarova, I. Lukes, T. Godula, I. Svobodova, P. Taborsky, J. Havel, Chem. Eur. J. (2003) 9233;
 (d) D.Y. Kong, A. Clearfield, Chem. Commun. (2005) 1005.

[19] (a) J.-G. Mao, A. Clearfield, Inorg. Chem. 41 (2002) 2319;
 (b) H. Jankovics, M. Daskalakis, C.P. Raptopoulou, A. Terzis, V. Tangoulis, J. Giapintzakis, T. Kiss, A. Salifoglou, Inorg. Chem. 41 (2002) 3366;
 (c) J.L. Song, A.V. Prosvirin, H.H. Zhao, J.-G. Mao, Eur. J. Inorg. Chem. (2004) 3706;
 (d) J.L. Song, H.H. Zhao, J.-G. Mao, K.R. Dunbar, Chem. Mater. 16 (2004) 1884.